Ince, E. S., Förste, C., Barthelmes, F., Pflug, H., Li, M., Kaminskis, J., Neumayer, K., Michalak, G. (2020): Gravity Measurements along Commercial Ferry Lines in the Baltic Sea and Their Use for Geodetic Purposes. - Marine Geodesy, 43, 6, 573-602.

https://doi.org/10.1080/01490419.2020.1771486

Gravity Measurements along Commercial Ferry Lines in the Baltic Sea and their Use for Geodetic Purposes

ABSTRACT

In 2017 and 2018 GFZ performed two gravimetry campaigns on commercial ferries in the Baltic Sea. The nature of such "non-dedicated" campaigns is different from "dedicated" campaigns that are performed on research vessels with tracks planned according to gravity measurement needs. The non-dedicated campaigns use non-survey vessels or survey vessels running for other purposes such as hydrographic measurements, which may require additional corrections. To assess the usefulness of non-dedicated campaigns, we analysed gravity measurements collected on two commercial ferries as part of the EU funded FAMOS project. Besides the typical marine gravimetry corrections, we also investigated the corrections for the vertical accelerations due to the ship's movement and the dynamical effect due to the cross-coupling between horizontal and vertical acceleration components. Taking the latter two corrections into account partly leads to slight improvements, but our results also demonstrate that the standard processing without the two corrections, as used in most of the dedicated campaigns, already delivers good quality end products that fulfil the requirements of a typical marine gravimetry survey with an uncertainty of about 1 mGal. Our findings suggest that gravimetry campaigns on commercial ferries can be used to complement dedicated marine gravimetry campaigns and contribute to geodetic purposes.

Keywords: Shipborne gravimetry, ferry gravimetry, Baltic Sea, FAMOS project, Chekan-AM, kinematic vertical acceleration

1- Introduction

The GFZ German Research Centre for Geosciences performed two gravity measurement campaigns on ferry lines between Travemünde and Liepaja in October 6-13, 2017 and Travemünde and Helsinki in October 29 – November 6, 2018. These ferry campaigns aimed to support the outcomes of the FAMOS (Finalising Surveys for the Baltic Motorways of the Sea, http://www.famosproject.eu/famos/) project by collecting records along very long lines in a cost-efficient way. Another aim was to test the gravimeter in environments where optimum measurement conditions were not met and see whether measurements on such non-dedicated campaigns could provide comparable information to complement dedicated gravity campaigns. To our knowledge, this is the first time it is investigated whether gravity measurements performed on commercial ferries can provide benefit to geodetic science on a large-scale and multidisciplinary project.

One of the fundamental goals of the FAMOS project is to improve the geoid model over the Baltic Sea. A high accuracy geoid model is an important basis for future offshore 3D-navigation and is also crucial for the on-going efforts of the Chart Datum Working Group (CDWG) of the Baltic Sea Hydrographic Commission (BSHC) (http://www.bshc.pro/working-groups/cdwg/) to introduce the European Vertical Reference System (EVRS) as a chart datum in the Baltic Sea (Nordman et al. 2018). The transition to a common chart datum in the Baltic Sea will be via a ~5 cm accuracy gravimetric geoid model (Ågren et al. 2016a, 2016b, 2019). Therefore, marine gravity measurements and geoid modelling are crucial components of this project.

Since 2014, about 20 “dedicated” and non-dedicated (piggy-back) shipborne gravimetry campaigns have been performed in the Baltic Sea by different institutions and agencies which aimed various scientific outcomes (Bilker-Koivula et al. 2017, Nordman et al. 2018, Varbla et al. 2017, 2020). Dedicated campaigns here refer to campaigns that were performed on research vessels with track plans designed according to the gravity measurement needs. In such vessels, the centre of mass and the centre of rotation of the ship, and the relative positions of the gravimeter (gravity sensor) and the GNSS antennae within the vessel’s local coordinate system would be very accurately known. On the contrary, non-dedicated campaigns refer to campaigns where the ship would run for other purposes such as hydrographic measurements or, in the case of ferry campaigns, for commercial shipping and transportation. On such ships, gravity measurements would be collected regardless of the measurement conditions which brings a risk of obtaining products with worse quality.

Within the FAMOS project, GFZ had various campaigns together with two German agencies, the Federal Maritime and Hydrographic Agency (BSH) and the Federal Agency for Cartography and Geodesy

(BKG), on BSH's survey, wreck search, and research ship Deneb (Johann et al. 2020; Lu et al. 2019). The campaigns performed on the Deneb were dedicated campaigns and aimed to cover the German waters densely (see **Figure 1**). Two ferry campaigns on the contrary were non-dedicated campaigns and are the topic of this study.

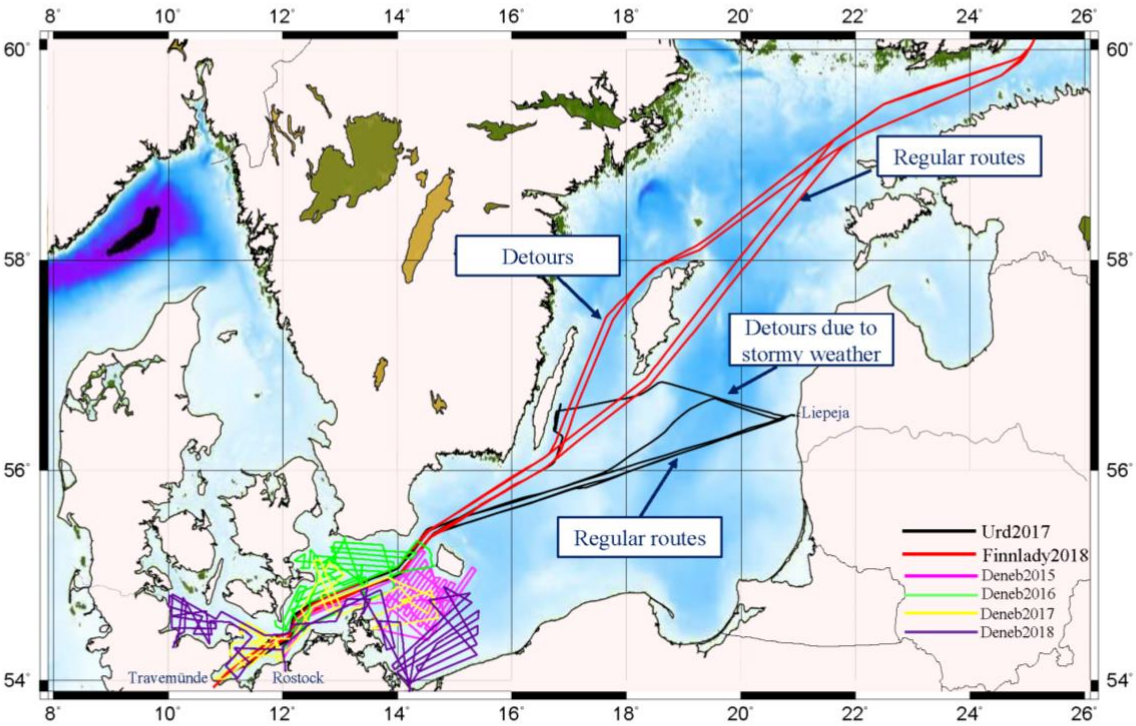

Figure 1. Measurement tracks covered in the two ferry campaigns, Urd2017 and Finnlady2018 and the dedicated campaigns performed on the German research and survey vessel Deneb.

In this study we used a traditional mobile gravimeter Chekan-AM, manufactured by CSRI Elektropribor (http://www.elektropribor.spb.ru/en/). Since its purchase in 2011, this Chekan-AM is the main equipment in GFZ's shipborne and airborne gravity campaigns, and it was used in the ferry campaigns presented in this paper as well. Atom interferometry measurements can provide absolute marine gravity measurements without the operational constraints of relative gravity measurements such as the necessity of repeating measurements at harbour tie points as well as the drift and calibration error of the instrument (Bidel et al. 2018). The first shipborne test measurements of atom interferometers showed promising results. Similar measurements have also been performed for airborne gravimetry providing comparable results w.r.t. ground upward continued gravity disturbances (Bidel et al. 2020). Nevertheless, more testing and developments are required before atom interferometers can be used outside of mobile lab environments and become cost-efficient for world-wide use. Therefore, researchers will continue to use and improve instruments and data processing strategies of the traditionally used mobile gravimeters (e.g. Chekan-AM and strap-down gravimeters) to accomplish mGal or sub mGal accuracy.

In mobile gravimetry, which includes airborne and shipborne gravimetry, inertial forces generated by the vessel motion are several orders of magnitude larger than the gravity signal. The gravity accelerations along the planned tracks are measured together with other motions and need to be post-processed to eliminate/reduce influences other than the gravity source. In marine gravimetry, the inertial forces and gravitational field can be separated by filtering the data since the inertial motions are mostly affecting the higher frequencies. However, in the measurements performed on ferries, which are much larger than typical survey vessels, the nature of the inertial forces may differ due to the size of the ship, long measurement tracks, higher speed, and larger speed variations compared to the survey vessel campaigns. Therefore, the data processing may need to be adjusted or precise measurements of the inertial acceleration may need to be performed.

In this paper, we investigate two corrections that are additional to our routine shipborne gravimetry data processing. These corrections are called the kinematic vertical acceleration correction and the dynamical cross-coupling effect correction. The first is related to the vertical movement of the survey vessel and the second is related to gyro stabilisation errors of the gravimeter due to the ship's movement. For the kinematic vertical acceleration correction, we investigate the use of GNSS-derived kinematic vertical accelerations to remove the effect of inertial accelerations from the gravimeter measurements as is done e.g. in GFZ's airborne gravimetry data processing (Petrovic et al. 2016, Lu et al. 2017). Our previous investigations show that the kinematic vertical accelerations retrieved from the GNSS measurements after filtering (400 second or even longer) should be better than 0.1-0.2 mGal accuracy to improve the gravimeter measurements. The dynamical effect during instant turns and abrupt speed changes is eliminated by manually checking and removing data, and it is investigated whether the dynamical effect correction in the rest of the tracks during the cruise is necessary. Apart from these corrections, instrumental drift was removed, and the gravity measurements were tied to absolute gravity measurements. The final products are compared to results from dedicated campaigns at cross-over points.

The aim of the paper is to investigate whether the accuracy of the final products is comparable to the dedicated campaigns which have higher costs. If so, this supports extending the use of non-dedicated campaigns to validate other campaign measurements and to contribute to the geoid calculation studies for the Baltic Sea. In the rest of the paper, we cover the following. In Section 2, we describe the ferry campaign organisational arrangements, the raw Chekan-AM records and gradient measurements in the harbours for tying the measurements to absolute gravity measurements. Section 3 covers the data processing which includes low-pass filtering, drift estimation and measurements. In Section 4, we present results from the two campaigns and analyses of crossover point differences w.r.t three dedicated campaigns. Finally, in Section 5, we conclude the paper.

2. Marine Gravity Measurements on Ferries

2.1. Ferry Campaigns

In dedicated gravimetry campaigns, there are many aspects that are taken into account while planning the measurement tracks. Filling patchy areas to improve local and regional geoid models and to harmonise old measurements that are referred to different reference values and processing schemes are two of the most common reasons to plan dedicated shipborne campaigns. Contrary to the dedicated gravimetry campaigns, ferry campaign measurements are spatially restricted to the predetermined ferry lines between two harbour points. The ferry campaigns that GFZ performed, Urd2017 and Finnlady2018, aimed to cover the longest tracks possible in the Baltic Sea which helps to identify discrepancies among earlier measurement campaigns and harmonise these with historical gravity measurements to study the geoid in the Baltic Sea. The tracks covered in the two ferry campaigns as well as in four dedicated Deneb campaigns performed together with BKG and BSH are shown in **Figure 1**. The tracks shown in **Figure 1** cover part of the FAMOS project area. The FAMOS project aimed to cover the entire Baltic Sea with similar campaigns performed by different project partners and is complementary to other studies such as geoid evaluation (see Ågren et al. 2016a, 2016b, 2019, Bilker-Koivula et al. 2017, Johann et al. 2020, Lu et al. 2019, Varbla et al. 2017 and 2020).

Both ferry campaigns consist of six tracks: 3 tracks from Travemünde and 3 return tracks from the corresponding harbours, Helsinki for the Finnlady and Liepaja for the Urd campaigns. The first tracks from Travemünde are influenced in both cases by the warming period of the instrument and are not included in data processing. Also, the last returns from Helsinki and Liepaja are not complete tracks since the deinstallation of the instrument had to start already during the cruise because of the limited times on arrival in the harbour. In the Finnlady case the second track (Helsinki to Travemünde, data collected after the warming of the instrument) is also not included in the final data processing since it was found to be much noisier than the following tracks (see Section 2). Even though the ferry line travels back and forth between the harbours, it is worth recalling that the measurements, apart from the tracks near the harbours, were not recorded on exact repeating tracks (see in **Figure 1**). Hence, the repeatability of the measurements cannot be analysed based on the collected records along such inexact return tracks. Instead, for validation purposes, we use internal and external crossover point differences which are presented in Section 4.

The total track length of the Urd campaign is around 4300 km, whereas it is about 5400 km for the Finnlady campaign which includes detours taken due to stormy weather (see **Figure 1**). Such long tracks, different sea and weather conditions and the oscillating motion of both ferries provide an opportunity to evaluate the instrument characteristics and measurement quality as well. The two vessels used in the ferry campaigns, namely Stena Line's Urd and Finnlines' Finnlady, have different characteristics from typical survey vessels and from each other. In terms of ship movements and corresponding stabilisation systems, they respond to the water and weather conditions differently. Moreover, some of the usual gravimetry requirements such as installation of the gravimeter at or close to the centre of the mass of the vessel were also not met since an appropriate space where the gravimeter could be set up properly is rarely accessible on such commercial RoPax ferries. On the other hand, contrary to the smaller size survey vessels, we expect more quiet sailing on such large ferry liners.

Photos of the two ferries and the equipment used in the campaigns are presented in **Figure 2**. The installation started upon the team's arrival to the ferries. The Chekan-AM gravimeter was installed on a higher deck that was about 15 metre (onboard Urd) resp. 28 metre (onboard Finnlady) above the harbour reference point and the two GNSS antennae are installed at the bridge level (**Figure 2**d). To prevent any interruption, the Chekan-AM gravimeter was installed in special rooms (see **Figure 2**c) in a crew-only area in both campaigns. Suitable cabins were advised by the ferry lines staff to meet requirements such as permanent access by the team and the ability to keep the temperature within a pre-defined range to ensure that the instrument does not deviate from the expected drift behaviour. For both ferries, the rooms for the gravimeter were located in the front part of the ship on the highest deck, which is far from the centre of the mass.

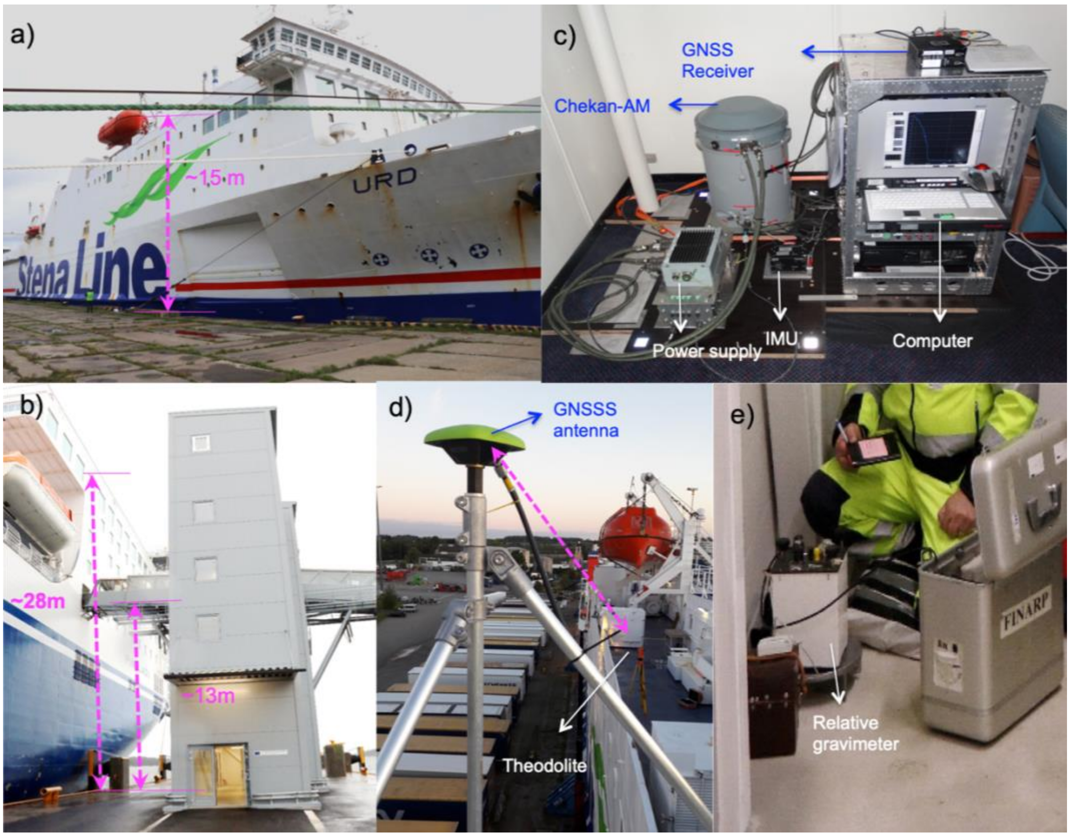

Figure 2. Equipment used in the ferry campaigns and impression of the field work (Photographs by GFZ): a) Stena Line's Ferry URD in the 2017 campaign. Note the Chekan-AM sensor height is ~15m above the harbour tie point, b) the reference harbour measurements that included height and gravity gradient measurements in Helsinki Vuosaari Harbour during the Finnlady2018 campaign, c) the Chekan-AM installation on URD. Note the other equipment such as IMU and power supply unit which were also installed on the same platform, d) The GNSS antenna on URD. Note the total station in the background that was used to establish a ship reference frame, e) relative field gravimeter used by Finnish Geospatial Institute (FGI) in Vousaari to carry from the absolute gravity value to the harbour inside the terminal tower.

2.2. Raw Gravity and Gradient Measurements

2.2.1. Raw Chekan-AM measurements

The working principle of the Chekan-AM gravimeter is based on the measurements of the angle variations of a double quartz elastic torsion system that is positioned in a viscous damping liquid. This (double) sensor system is supported by a temperature stabilisation and a gyro stabilisation system. The gravity sensor unit is mounted on a gyro stabilised platform that is kept horizontally using six one-axis floating gyros. Additionally, accelerometers provide feedback to the internal system. This platform ensures that the sensitive axis is held in the vertical direction. The details of the instrumentation and the data processing routine recommended by the manufacturer can be found in Krasnov et al. (2011a and 2011b) and in the Chekan-AM Operating Manual. The raw measurements of the Chekan-AM gravimeter are integer numbers of pixels detected on two CCD photodetectors which represent (by two light beams) the relative positions of the two sensor masses in terms of angles. The pixels are converted into acceleration units using transformation parameters provided by the manufacturer (Krasnov et al. 2011a, Zheleznyak et al. 2009). The transformation parameters are based on the position and the rate of change of the position (first derivative).

Figure 3 shows examples of raw instrument readings in terms of pixel position, as well as in terms of the acceleration unit. The longitudinal and transversal accelerations measured by the accelerometers of the longitudinal and lateral axes of the gyro stabilisation system, and the roll and pitch angles, retrieved from the accelerometers mounted in the gyro platform, are shown in the same figure. The right and left columns of **Figure 3** show measurements from almost repeating tracks; therefore, one may expect to see similar signal behaviour moving in the opposite direction along the measurement path. However, the measurements between Helsinki and Travemünde (left column) show high noise segments which might be due to weather conditions or temperature instability of the viscous damping liquid. Therefore, this track is not included in the final delivered products.

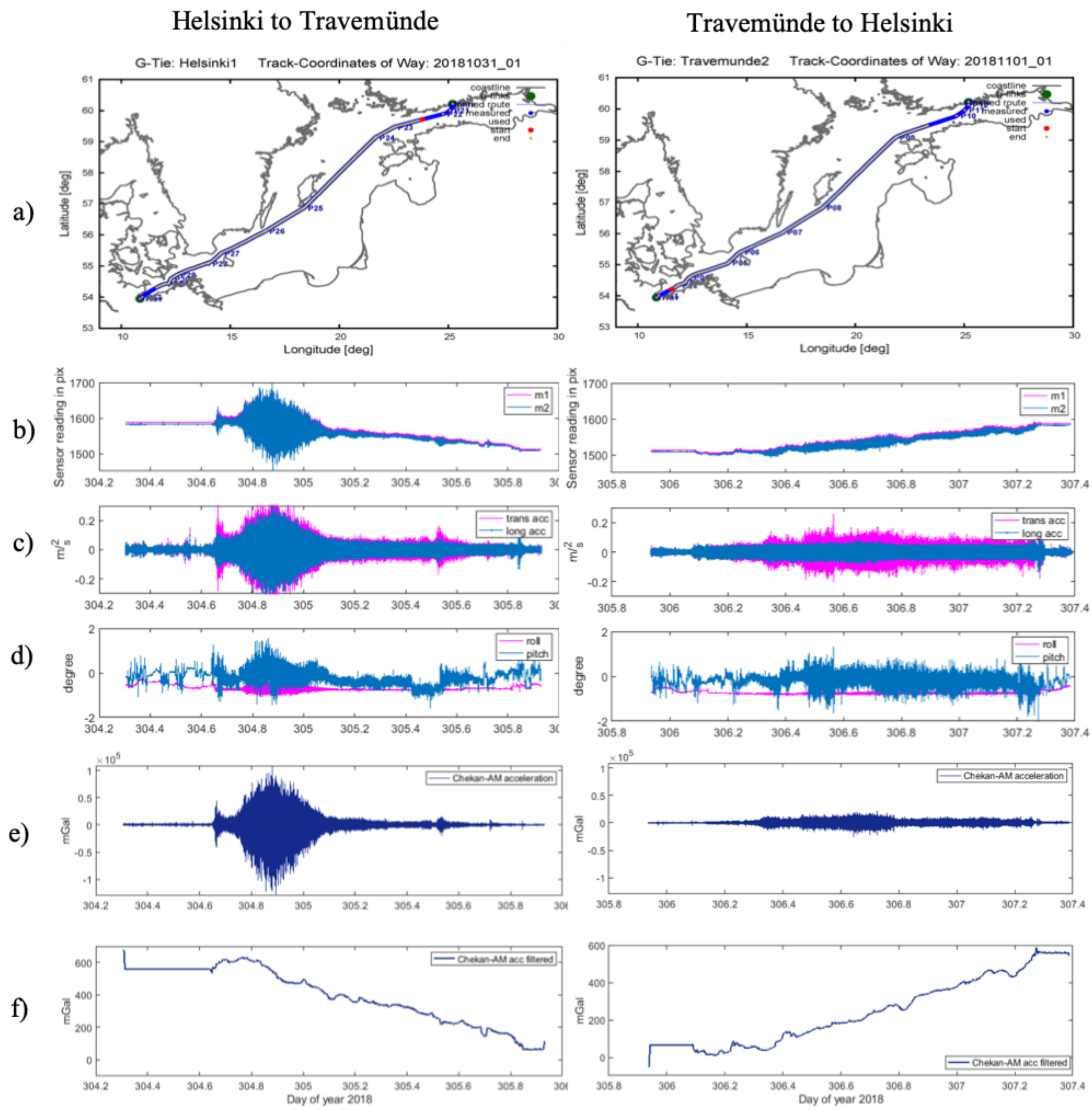

Figure 3. Finnlady 2018 measurements for the first two tracks after the recommended instrument warming period of 24 hours. The left column shows the measurements for the track between Helsinki and Travemünde, whereas the right column shows the following track between Travemünde and Helsinki. The six rows depict a) The coordinates of the measurement tracks, b) original readings from the two individual sensors of the double quartz elastic torsion system inside the Chekan-AM in terms of pixel positions, c) translational and longitudinal accelerations, d) roll and pitch angles. Note that c) and d) are retrieved from the Chekan-AM gyro stabilisation system. e) The measurements converted into acceleration unit, f) the same as in e) but low-pass filtered to reduce the high frequency noise components. (The Eötvös correction is not applied yet to the measurements presented in row f). Note different ranges in the y axes in e) and f)

2.2.2. Local tie and vertical gradient measurements in harbours

Measured gravity values in mobile gravimetry are not absolute gravity values but gravity variations along the track. Thus, they need to be connected to an absolute gravity value at harbour tie points which requires additional measurements on land. As shown in **Figure 4**, land measurements include the relative gravity measurements between an absolute gravity reference station and the harbour tie point, vertical gravity gradient measurements at the harbour tie point, as well as the height difference measurements between the harbour tie point and the gravimeter sensor point on the ferry.

In order to transfer (reduce) the absolute gravity value to the height of the gravimeter sensor point, the height difference between the harbour tie point and the gravimeter sensor point (**Figure 4**) was measured using a total station, while the corresponding vertical gravity gradient value at the harbour tie point was measured using a relative field gravimeter. As commonly practised, to obtain the vertical gravity gradient, gravity was measured at the Earth's surface and at a height of about 1 metre at least (see **Figure 5**). It is worth noting that, as proposed by other scientists, we tried to transfer the absolute gravity value directly from the harbour tie point up to the Chekan-AM by using a Scintrex CG-6 field gravimeter inside the ferries. We expected that such large vessels may be sufficiently quiet in the port. However, this method has failed since the swaying of the ship was too strong.

In the dedicated shipborne gravimetry campaigns of the FAMOS project, the measurements were generally performed in research vessels, such as BSH's Deneb (Johann et al. 2020; Lu et al. 2019) where the coordinate system and centre of mass (and rotational centre) of the vessel are known or precisely measured. Furthermore, in most cases the gravimeter was located at or close to the centre of the mass of the ship which was also close to the actual sea level and the tie point in the harbour. Therefore, the height difference between the gravimeter sensor and the reference tie point generally would not exceed ~1 m. Accordingly, when measuring on such survey vessels, it is not necessary to measure the gravity gradient to tie the measurements at gravimeter sensor point to the absolute gravity value at the harbour since the difference between the real gradient and the mean free-air gravity gradient has a negligible effect for a vertical separation below 1 m. Thus, in these cases, the free-air gravity gradient value (0.3086 mGal/m) was used to transfer the absolute gravity value to the gravimeter sensor point in the past.

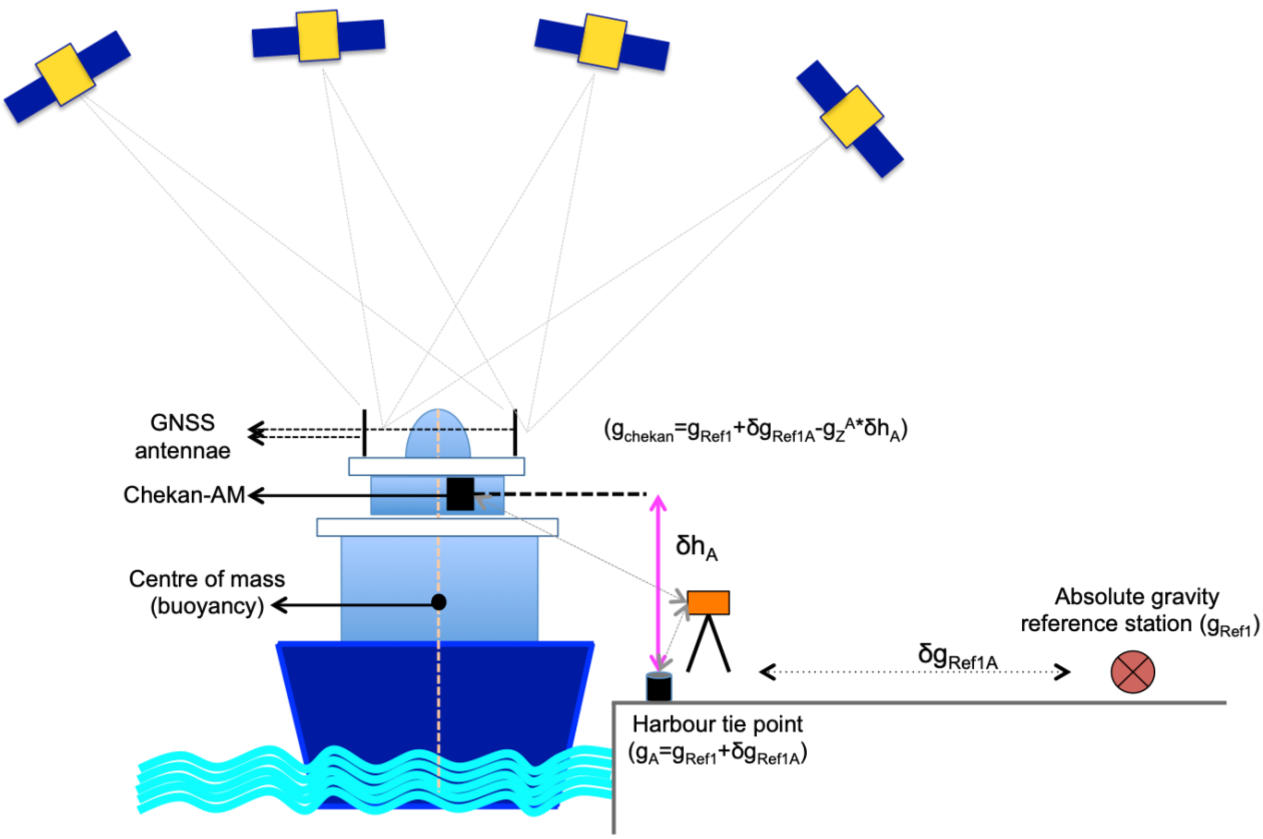

Figure 4. The scheme of gravity reference and harbour measurements. The harbour gravity value is carried from the absolute gravity reference station using a relative gravimeter. The tie point reference value is reduced (transformed) to the Chekan-AM sensor using the height and radial gravity gradient measurements in the harbours.

Figure 5. Vertical gradient measurement arrangements at harbour tie points a) on a large concrete bollard in Travemünde, Finnlady2018 and b) on a dedicated gradient tripod in Liepaja, Urd2017 (Photographs by GFZ).

In the Urd2017 case, our team experienced for the first time the need to perform gradient measurements since the gravimeter sensor platform in the ferry was located about 15 m above the harbour reference tie point (see **Figure 2**a). Hence, the question was raised whether the commonly used mean vertical free-air gravity gradient is still good enough for transferring the absolute gravity value from the tie point to the gravimeter sensor point or whether we need to measure the gradient for each harbour tie point in such campaigns. In our second ferry campaign Finnlady2018, the height difference between the Chekan-AM sensor point and the harbour tie point was about 25 to 28 m. Dedicated gradient and height measurement sessions were planned to introduce precise vertical gravity gradients to tie the Chekan-AM measurements to the reference gravity value at the harbour point. It is worth noting that the Latvian gravimetric support points, previously validated during the Danish – Baltic Sector Program 1996-1998, were used to link the Chekan-AM gravity measurements to the absolute gravity reference stations.

The summary of the absolute gravity values and vertical gravity gradients measured at the harbour tie points with their coordinates is presented in **Table 1**. Two relative gravimeters ZLS Burris (Jentzsch et al. 2018) and Scintrex CG6 (Scintrex, 2018) were used for the gradient measurements. In the Finnlady case in Travemünde, it was possible to measure the gradient on a large concrete bollard at 2.2 metre height and in Helsinki over a much larger height difference of about 13 metres inside the terminal tower on the peer beside the vessel (see **Figure 2**b).

Table 1. Absolute gravity values transferred to harbour tie points and vertical gradients at the reference harbour tie points used in the Urd2017 and Finnlady2018 campaigns and their error estimates. The absolute gravity values are transferred to the Chekan-AM sensor point using the actual (i.e. loading dependent) height differences measured between the sensor and harbour tie point at each arrival and departure. The absolute gravity value in Travemünde at Pier 3 was measured by BKG, in Liepaja it was carried from the absolute gravity reference point by GFZ in cooperation with Riga Technical University and in Helsinki it was carried from the absolute gravity reference point by Finnish Geospatial Research Institute (FGI). The gravity gradients for Liepaja (Fig. 4b), Helsinki (Fig. 2b) and on Pier 6 at Travemünde (Fig. 4a) were measured by GFZ. BKG delivered the gradient value for Pier 3 at Travemünde.

	Urd2017		**Finnlady2018**	
	Liepaja (Pier 46, GFZ)	Travemünde (Pier 3, BKG)	Helsinki (Pier CP, FGI/GFZ)	Travemünde (Pier 6, GFZ)
Latitude (degree)	56.527543	53.949053	60.219240	53.942680
Longitude (degree)	20.993834	10.858088	25.199242	10.860806
Reference value (mGal)	981629.035 +/- 0.030	981414.356 +/- 0.010	981907.150 +/- 0.009	981412.245 +/- 0.069
Gradient Measured (mGal/m)	-0.334 +/-0.005	-0.327 +/-0.004	-0.311 +/-0.010	-0.307 +/- 0.012

To ensure an accuracy of 0.1 mGal for the gravity transfer along 20m in the vertical, the gradient must be known with an accuracy of 0.005 mGal/m. In the Liepaja example, the estimated gradient differs by 0.025 mGal/m from the usually considered mean free-air gravity gradient value. Such a difference would give a discrepancy of about 0.4 mGal for the 15 m height difference in case of Urd between the pier and the gravimeter reference point inside the vessel. This indicates that the gravity gradients should indeed be measured and considered in the data processing since we aim for an accuracy of about 0.5 to 1.0 mGal.

3. Data Processing

This section summarizes the data processing scheme of the shipborne gravity measurements which is followed by GFZ and which was also applied for the two ferry campaigns. The scheme is summarised in **Figure 6**. Different colours indicate different links between the input data and retrieved products in the data processing chain.

As it is one of the largest effects in mobile gravimetry, measurements collected on a moving platform need to be corrected for the Eötvös effect. Moreover, the gravity measurements need to be low-pass filtered to eliminate the high frequency noise (caused by e.g. the inertial acceleration) and the turning periods need to be scanned manually for potential large errors involved. The algorithms need to be modified based on the quality of the measurements and the measurement conditions, specifically the low-pass filter length, selection of the harbour measurements used in the drift estimation, and length of periods removed due to the large error around turning points. More details on each modification are given in this section.

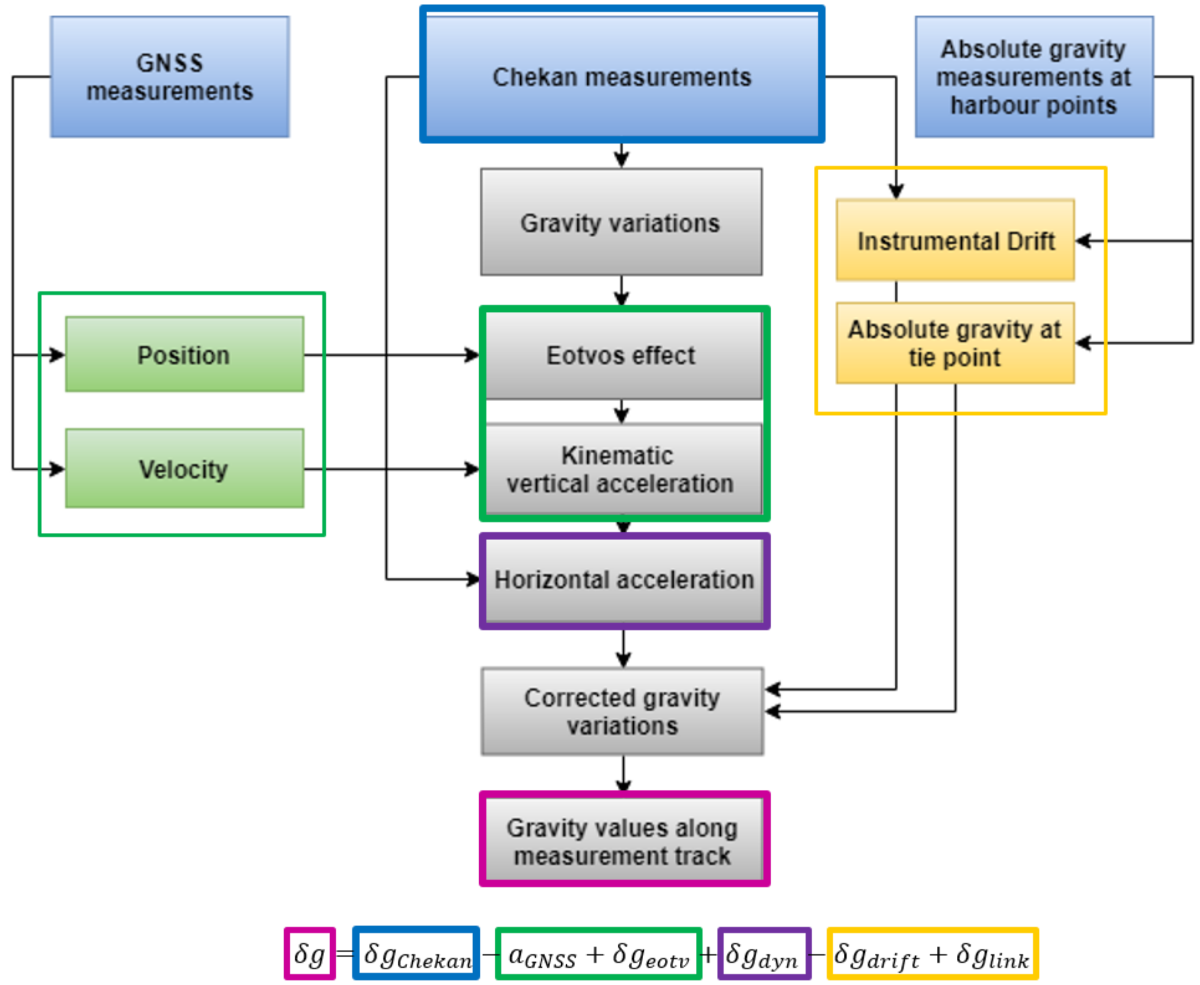

Figure 6. The data processing scheme of the shipborne gravity campaigns is shown here. In addition to the steps shown in this figure, the Chekan-AM measurements are converted into acceleration units and the GNSS-derived position and velocity (not direct GNSS measurements) are low-pass filtered in the beginning of the routine.

3.1. Low-pass Filtering

In our previous studies, a 400 second cut-off low-pass filter was generally used in the data processing (Barthelmes et al. 2016, Johann et al. 2020, Lu et al. 2019, Petrovic et al. 2012). However, the length of the filter must be adapted based on the equipment (e.g. survey vessel) as well as the measurement conditions. Therefore, for each campaign different low pass filters were tested which was also done in Lu et al. 2019. In our ferry campaigns, we tested 200, 300, 400, 600, 800, and 1200 seconds filter lengths. The choice of the filter length should be a compromise between good spatial resolution and good noise suppression.

According to Krasnov et al. (2014), the RMS value of crossover point differences of a marine gravity survey typically ranges between 0.2 and 0.8 mGal, which primarily depends on the sea condition. Depending on the measurement conditions and the speed of the vessel, the spatial resolution of such surveys varies from 300 to 1500 m (half wavelength). The average speed of Urd was about 14.8 knots (~ 7.7 m/s), whereas Finnlady's was about 22 knots (~11 m/s), which causes the spatial distance between each measurement on the Finnlady to be larger. Based on the crossover point differences between Urd2017 and three dedicated campaigns (see also **Table 2**), 300 second and 400 second cut-off low-pass filters deliver about similar RMS, whereas other filter lengths deliver worse results (not provided in the table). To be consistent with our previous campaigns, we applied a 400 second cut-off low-pass filter in the Finnlady data processing too, which delivers a spatial resolution of about ~ 2 km half wavelength.

3.2. Drift Estimation

One of the most challenging tasks of relative gravimetry is dealing with instrument drift. The drift has to be computed as good as possible based on repeating harbour measurements and taken into account in the data processing. Due to the aging of the sensors as well as the characteristics of the equipment used in the instrument's development, such as the viscous damping liquid, it is necessary to calibrate the Chekan-AM gravimeter about every three years. Because of anomalous drift behaviour, the original sensor unit of GFZ's Chekan-AM gravimeter was replaced in 2017 before the ferry campaigns. Bench tests performed by the manufacturer showed that the original gravimeter sensor was subject to about 3 mGal/day drift (see Chekan-AM Operating Manual). Based on the measurements performed in our lab, the new sensor set is subject to a smaller drift of about 0.2 mGal/day. Accordingly, after the replacement of the original instrument sensors, we expect to receive and deliver higher quality gravity measurements in our campaigns from 2017 and 2018 than in earlier campaigns.

However, the drift estimate in the lab environment is not sufficient to use in the actual processing. The drift has to be computed as good as possible based on repeating measurements at harbour tie points so that it can be eliminated in the data processing. In our ferry campaigns, correction for the drift (or null-point drift) was determined from the results of repeated measurements at the same reference harbour or different harbours in which the absolute gravity values are known. Measurement of the sensor height with respect to the reference point is particularly important for the drift calculation. What makes the height measurement and the gravimeter measurement at the harbour challenging is the effect of the loading and unloading of the trucks during the ferry's stay at the harbour. The loading/unloading effect is mainly manifesting in height changes of the gravimeter sensor w.r.t. the harbour pier. Hence, the gravity and height measurements should be associated with the arrival and departure times precisely in the repeating harbour measurements due to the height changes because of the loading/unloading effect. Therefore, we did the height measurements on each arrival and departure as well as between in the respective stay in the harbours. We noticed height variations up to one metre caused by different loading. Such height differences correspond to gravity variations of about 0.3 mGal which is relevant to be considered for drift estimation. On the contrary, the attracting effect of the masses of the load (lorries/trucks) is negligible in this example.

To reduce the possible error that usually a measurement at a single epoch may introduce, we take the average of several hundred or thousand seconds Chekan-AM gravity measurements at the harbour to connect the relative gravity measurements to the reference value. The absolute gravity values transferred to the Chekan-AM measurement sensor point (see **Figure 4**) for the two harbours are obtained as: $g^A_{chekan} = g_A - g^A_z \delta h_A$, and $g^B_{chekan} = g_B - g^B_z \delta h_B$, where g_A and g_B are absolute gravity values, and g^A_z and g^B_z are the corresponding vertical gravity gradients measured at the harbour tie points.

The drift between the two reference points is then computed via: $\delta g_{drift} = \frac{[(g^B_{chekan} - g^A_{chekan}) - (\overline{\Delta g}^B_{chekan} - \overline{\Delta g}^A_{chekan})]}{\Delta t}$ where $\overline{\Delta g}$ refers to the average of harbour measurements and Δt represents the time difference between the corresponding epochs of harbour measurements used in drift estimation.

For the sake of high-quality measurements, the temperature has to be monitored and controlled during the entire measurement period. After the gravimeter is installed and switched on, the viscous damping liquid inside the Chekan-AM has to be within the predefined temperature range before taking measurements. In both campaigns, we analysed the measurements after completion of the recommended 24-hour warming period. The computed drift estimates are shown in **Figure 7**a and b, for Urd2017 and Finnlady2018, respectively.

From our previous experiences and based on the Operational Manual of the instrument, we expect a positive linear drift behaviour. The estimated drift value for Urd2017 is in a very good agreement with the drift estimated in our labs. However, in the Finnlady example, the drift calculated from the first two harbour measurements showed a negative behaviour. Since from our previous experiences we know that the drift is negative in the warming-up phase, we think that the replaced sensors may require a longer warming period. To ensure high quality measurements, we computed the drift without the first harbour measurements in Helsinki and did not include the first track back to Travemünde, which is also shown in **Figure 3** (left column), in the delivered products. We compute a linear drift rate of about 0.683 mGal/day based on the remaining harbour measurements which is similar to the drift behaviour of our dedicated campaigns. Therefore, this value is used in our analyses. **Figure 7**b summarises the drift estimates and measurements used for its estimation. The (formal) uncertainty of the drift can be derived from the noise of the used data.

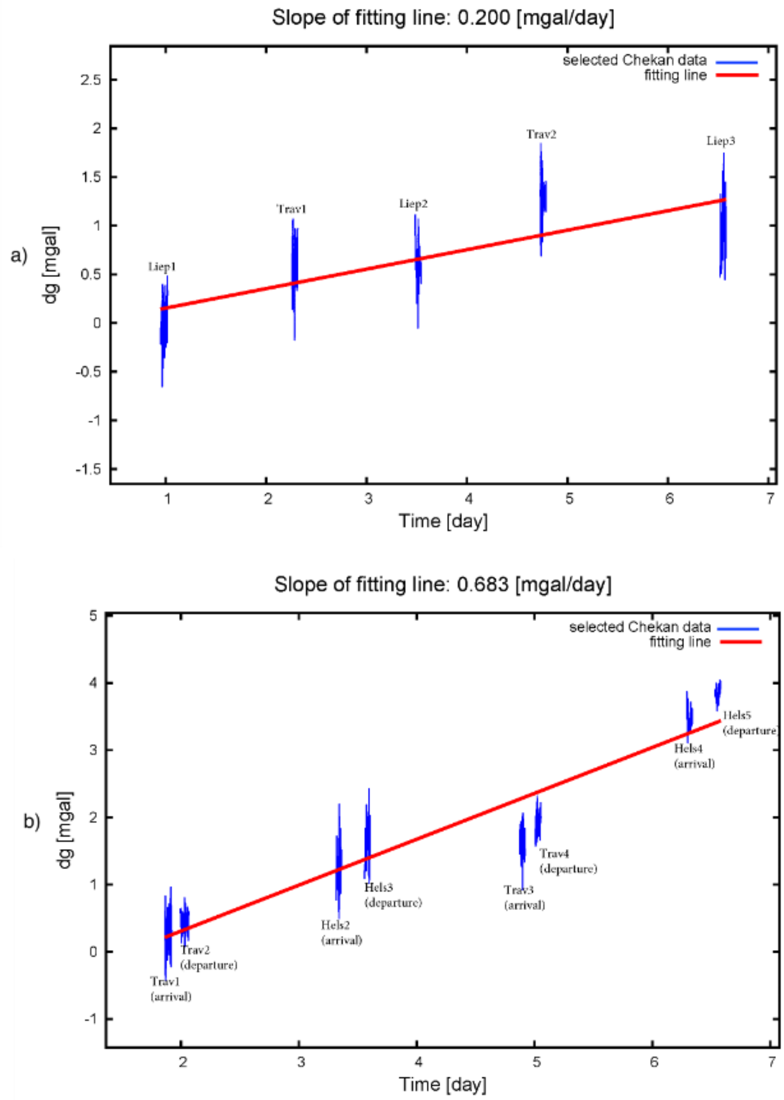

Figure 7. Drift estimate of the Chekan-AM during the two ferry campains, a) Urd2017, b) Finnlady2018. Note in the Finnlady case, both arrival and departure time series in the harbour are used in the drift calculation whereas in the Urd only the departure time is used since the difference was not significant. Time on the x axis corresponds to the day of the relevant campaign.

We did not calculate the uncertainty of the estimated drift because possible errors from other sources (e.g. vertical position of the gravimeter in the harbour) are not known. However, to try and quantify the uncertainty in the drift estimates, we did some comparisons with high resolution global gravity field models. The Chekan-AM computed gravity disturbance variations along the 5 tracks are compared with EIGEN-6C4 (Förste et al. 2014) computed ones. The differences (residuals) between the two are investigated to check whether the trend of the residuals can represent the drift behaviour of the instrument. In this way, it is possible to calculate the drift independently from the harbour measurements. However, in our case the drift calculation based on differences with respect to EIGEN-6C4 was highly sensitive to gravity measurements considered in the drift calculation. Therefore, we think that the drift estimation based on harbour measurements is still more reliable in our ferry campaign examples and was therefore preferred in the final data processing.

3.3. Measurements

3.3.1. GNSS records

Gravity measurements should be presented together with the position information for each epoch. In our campaigns, we include at least two GNSS antennae located at the best positions possible (see **Figure 2**d and **Figure 4**). The positional trajectories of the vessels are computed based on the measurements of each GNSS antenna using GFZ's Earth Parameter and Orbit System (EPOS-OC) software package (www.gfz-potsdam.de/en/section/global-geomonitoring-and-gravity-field/topics/earth-system-parameters-and-orbit-dynamics/earth-parameter-and-orbit-system-software-epos/) by applying a standard PPP (Precise Point Positioning) approach. The original GNSS observation and gravimeters reading rate is 10 Hz. The GNSS measurements are down-sampled to 1 Hz observation rate before processing via EPOS.

In our application, which concerns a moving platform in the Baltic Sea, we model the tropospheric delay of the GNSS signal using a standard atmosphere together with the Vienna Mapping Function 1 ("VMF1", Böhm et al. 2006) including adjustment of a tropospheric scaling factor. If the solutions for the individual antennae are of similar quality, the average height information is used in the computation. In our routine data processing scheme the GNSS derived positions (coordinates) are spline interpolated to the gravimeter observation epochs for consistency. Additionally, in both dedicated and non-dedicated campaigns when its installation is possible, an inertial measurement unit (IMU) is used to retrieve the rotational angles of the ship. Such information can be used to monitor the quality of the gravity measurements collected. It is worth noting that the lever arm effect is not taken into account in our routine data processing since it is assumed to be small after applying the 400 seconds cut-off low pass filter.

In the Urd2017 campaign, we installed two Javad GNSS antennae on-board the ferry that measure the position. The ellipsoidal height information provided by the two antennae, calculated based on the above mentioned GFZ's EPOS-OC software tool, is shown in **Figure 8**a. In the next step, the height values are reduced to the gravimeter sensor point using the height differences measured by total station in the beginning of the campaign between the antennae and the Chekan-AM sensor point. Because the results from the two antennae are consistent, the average values of the two antenna heights that are reduced to the Chekan-AM sensor point is used in the data processing. Both antennae results indicate noisier periods during the last two days of the campaign especially in the Northern part of the Baltic Sea. These noisy signal characteristics occur close to Liepaja and are due to weather conditions. The height measurements for the Finnlady campaign are shown in **Figure 8**b. Due to the higher deck of the Finnlady, the antennae heights are about 10 m larger than for the Urd.

In addition to the coordinate information, which is recorded to position the gravity measurements, velocity and acceleration information are also needed in the calculation of the kinematic vertical accelerations (see **Figure 6**). For this purpose, we used an alternative processing solution than used in EPOS. In our solution, the GNSS based velocity and acceleration values are calculated from time-differencing of the carrier-phase measurements (Li et al. 2019). The L1 observable is used because of its lower noise compared to the ionosphere-free linear combination observation. Based on the PPP observation model, the L1 observation is numerically differentiated to obtain both range rate and range acceleration. The troposphere and ionosphere delay errors are highly time correlated and can be mitigated over a short time interval (less than or equal to two seconds). Furthermore, in the case of our ferry campaigns, the GPS and GLONASS observations are used to enhance the reliability of the solutions. The satellite clock drifts, and drift rates are derived from the GFZ analysis centre final products.

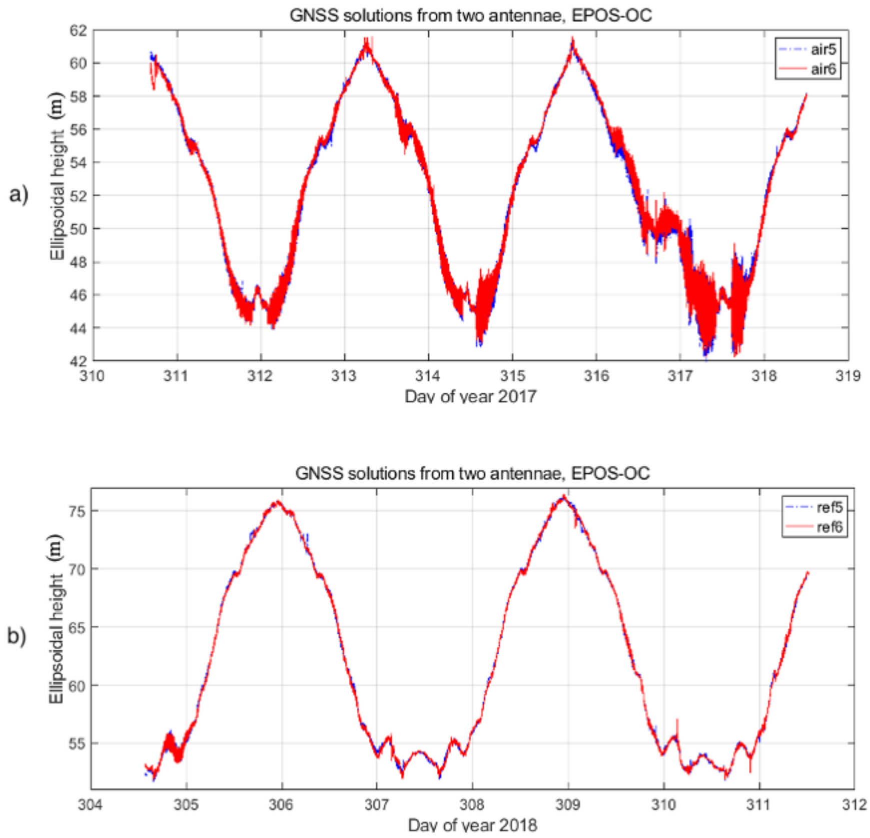

Figure 8. GNSS ellipsoidal heights retrieved using GFZ's EPOS-OC GNSS software tool, a) Urd2017 GNSS ellipsoidal heights for both antennae at the antenna heights. They are distinguishably noisier between days of year 316 and 318 due to the measurement conditions on these particular days. In the final processing, the averaged elevation values were used, b) Finnlady 2018 GNSS solutions for the height component from the two antennae. The averaged elevation values were used in the final data processing. The latitude and longitude time series also indicate similar noisy intervals for both campaigns.

3.3.2. Gravity records

The acceleration measurements do not solely consist of the gravity acceleration but also include the accelerations due to other sources such as the vertical movement of the vessel. The movement of the survey vessel, sea roughness, wind and temperature conditions have a strong impact on the gravimeter measurements. Measurements performed under optimum conditions during dedicated gravimetry campaigns may not require detailed investigations since applying a low-pass filter can reduce noisy signals already sufficiently. However, in the ferry campaigns unexpected drift behaviour and unknown sensor effects require detailed investigations and tests before high-quality and high-resolution spatial measurements can be retrieved. Specifically, we investigate the residuals after low-pass filtering and whether inertial acceleration source signals can be eliminated from the final gravity field products.

As mentioned above, our routine data processing scheme summarised in **Figure 6** follows the Chekan-AM Marine Operation Manual and Krasnov et al. (2011a). The formula to retrieve the corrected Chekan-AM (relative) gravity measurements can be written as:

$$\delta g = \delta g_{Chekan} + \delta g_{eotv} - \delta g_{drift} + \delta g_{link} - a_{GNSS} + \delta g_{dyn} \text{ , (1)}$$

where δg_{Chekan} is the raw gravity measurement recorded by the gravimeter, δg_{eotv} is the Eötvos correction (Jekeli, 2001), δg_{drift} is the Chekan-AM gravimeter drift correction, and δg_{link} is the gravity difference calculated between the Chekan-AM sensor point and the harbour tie point. In addition to the standard processing, we consider two specific error sources in this research, namely a_{GNSS}, the kinematic vertical acceleration computed from the GNSS measurements, and δg_{dyn}, the dynamical cross-coupling correction. The kinematic vertical acceleration correction (a_{GNSS}) is essential for airborne gravimetry but not for shipborne gravimetry data processing (e.g. Blazhnov, 2002; Krasnov et al. 2011; Krasnov and Sokolov 2015; Lu et al. 2017; Lu et al. 2019; Sokolov, 2011). Yet, the examples in the literature include only dedicated campaign examples, whereas the ferry campaign measurements by nature are exposed to different measurement conditions and to other disturbing behaviour. Hence, the kinematic vertical acceleration as well as dynamical effect corrections were investigated in this contribution for the ferry campaigns as formulated by Zheleznyak et al. (2009) and Sokolov et al. (2019).

Case studies on the calculation of the kinematic vertical accelerations for GFZ's marine gravity campaigns can be found in Li et al. (2019) and Lu et al. (2019). The dynamical effect correction which stems from instrumental imperfections is formulated as:

$$\delta g_{dyn} = \delta g_{HAC} + \delta g_{orb}. \quad (2)$$

The Harrison effect, δg_{HAC} arises from the projection of horizontal accelerations on the gravimeter's sensitive axis as a result of tilt caused by gyro stabilisation errors. It can be written as:

$$\delta g_{HAC} = W_x \alpha + W_y \beta, \quad (3)$$

where W_x is the longitudinal horizontal acceleration, W_y is the lateral horizontal acceleration, α and β are the angles of inclination of the sensitive element of the gravimeter due to the stabilisation errors. The orbital effect on the other hand is due to the combined action of the horizontal acceleration and the tilts of the gravimeter's sensitive axes caused by the vertical accelerations. This effect is also known as cross coupling effect. The summation of the readings of the two individual torsion systems helps to eliminate the orbital effect almost completely in the new type of Chekan-AM gravimeter (Zheleznyak et al. 2009). In our study, the orbital effect is computed from the direct sensor readings as:

$$\delta g_{orb} = k(m_2 - m_1)W_x, \quad (4)$$

where m_1 and m_2 are readings of the two sensors of the double quartz elastic torsion system, $k = 3.15$ x 10^{-5} rad/pix is the coefficient of transition from pixels to the angle of rotation of the quartz's systems pendulum provided by the manufacturer.

The first correction, namely the kinematic vertical acceleration correction for the two ferry campaigns is computed based on the velocities derived from the GNSS measurements and is presented in **Figure 9**a and 9b. After applying the kinematic vertical acceleration correction, there are cases where we observe reduction in the Chekan-AM measurement noise (Lu et al. 2019). However, the corrections may also introduce spurious signals if they are applied as a routine correction to the gravimeter records of the ferry campaigns. The two dashed lines shown in **Figure 9** indicate examples from the Finnlady2018 campaign where the corrections are not of satisfactory accuracy and introduce small jumps to the original signal. Consequently, apart from some particular purposes, such as the reduction of the effect of the seiches (standing waves that occur in an enclosed or semi-enclosed water body) that are also mentioned in Lu et al. (2019), introducing the kinematic vertical accelerations in the shipborne gravimetry routine data processing is not applied in our examples.

The second correction the dynamical effect correction, shown in **Figure 9**c is computed based on the Chekan-AM measurements. This correction can be interpreted as the correction for the residual effect of the cross-coupling of the horizontal and vertical acceleration which is largely but not completely eliminated by the design of the double quartz elastic torsion gravimeter principle. Eliminating the cross-coupling completely is not possible due to the imperfect instrumentation. As shown in **Figure 9**c, the residual effect is very small and has negligible impact on the final results. Therefore, we did not introduce this correction in the routine data processing either. Contrary to the two corrections mentioned above, the Eötvös correction shown in **Figure 9**e has a very significant effect and must be applied in mobile gravimetry as accurately as possible. A residual effect is discussed in the following section.

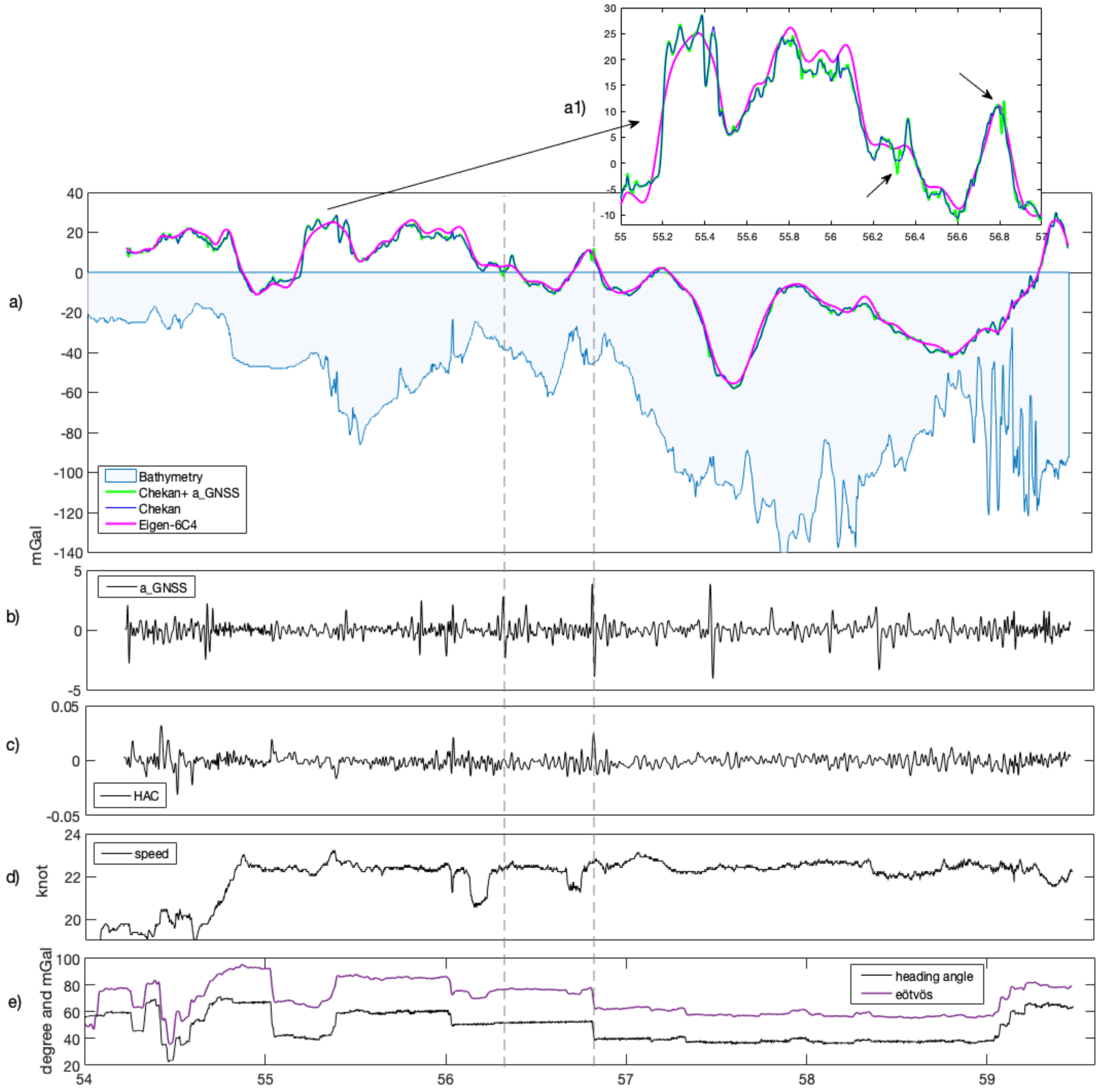

Figure 9. Final gravity disturbances and corrections applied: a) Chekan-AM final gravity disturbances are shown with and without the kinematic vertical acceleration corrections applied and are given together with the GEBCO bathymetry data (Weatherall et al. 2015) and EIGEN-6C4 computed gravity disturbances along the track. Note the disturbances introduced by the kinematic vertical accelerations (a_GNSS) for a small section are enlarged in a1), b) kinematic vertical accelerations derived from the GNSS measurements, c) dynamical effect correction, d) speed of the ferry retrieved from GNSS measurements, e) heading angle of the ferry and Eötvös correction both computed from the GNSS measurements.

3.4. Scanning the Final Products

As mentioned above, the Chekan-AM has a gyro stabilisation system, which makes it reliable to do measurements on moving platforms. However, the stabilisation is only in 2D and movement around the vertical axis (yaw) is not corrected using the Chekan-AM gyro system itself. Accordingly, there will be an effect from yaw motion of the vessel on the gravity measurements. Even though most part of this effect is removed via the Eötvös correction, the residuals need to be investigated. In addition to the yaw motion, rotational and translational motions need to be examined in order to analyse our ferry campaign measurements.

The heave (linear vertical motion) may be partly reduced using the GNSS derived kinematic vertical accelerations but remaining heave can leak into the final gravity measurements under strong heave conditions. Sway (the linear transverse, side to side or port-starboard motion) and surge (the linear longitudinal, front-back or bow/stern motion) are controlled by the water and wind conditions and may leak into our observations due to the working principle and position of the instrument. We learned from our previous campaigns that because of the yaw motion, the periods affected from turnings of the vessel need to be removed from the final gravity records. In most of the campaigns, we performed this elimination via manual edits by scanning the measurements over the turning periods already in the quick check procedure during the campaign on the ship.

It's worth noting that Finnlady contains a stabilisation system which gave a remarkable quiet environment for the gravity measurements onboard. Nevertheless, the gravimetry campaign performed on this vessel is a good example where the data had to be examined particularly for the turning periods and other disturbing acceleration events since their influence was found to be much larger due to the significantly higher speed and speed variations of this vehicle compared to URD and other survey vessels used in dedicated campaigns. These disturbed records were also manually scanned and removed from the final delivered gravity records.

In the Finnlady campaign, we could not install the IMU on board; therefore, the speed and heading angles shown in **Figure 9**d and 9e are retrieved from the GNSS measurements only and are used in our analysis for comparison purposes, which can give an insight whether the effect leaks into the final gravity measurements and/or the filter parameters need any modification.

4. Ferry Campaign Results

4.1. Summary of the Final Gravity Values in Terms of Gravity Disturbances

The outcomes of the two ferry campaigns are represented in terms of gravity disturbances in **Figure 10**. The gravity disturbances (Chekan-AM final gravity values minus WGS84 normal gravity computed at the gravimeter measurement point) are shown for the two campaigns together with the ETOPO 1min bathymetry (ETOPO) in the background. The gravity disturbances vary between -58.320 and 30.034 mGal in the Finnlady campaign, and between -25.710 and 31.486 mGal for the Urd campaign where the depth can reach up to about 160 m along the tracks. The turning periods close to the land and islands (e.g. Gotland) are investigated in detail and some sections have been removed as mentioned in Section 3.4.

For both datasets the kinematic vertical acceleration and dynamical effect corrections are not included in the final solutions since they do not enhance the overall accuracy of the results as discussed in section 3.3.2. In the Finnlady campaign, the measurements close to Helsinki harbour are not included in the final delivered products since these values are highly disturbed due to speed variations which were necessary because of the difficult sea floor topography in this region. We validate the campaign results by means of cross-over analyses in the following section.

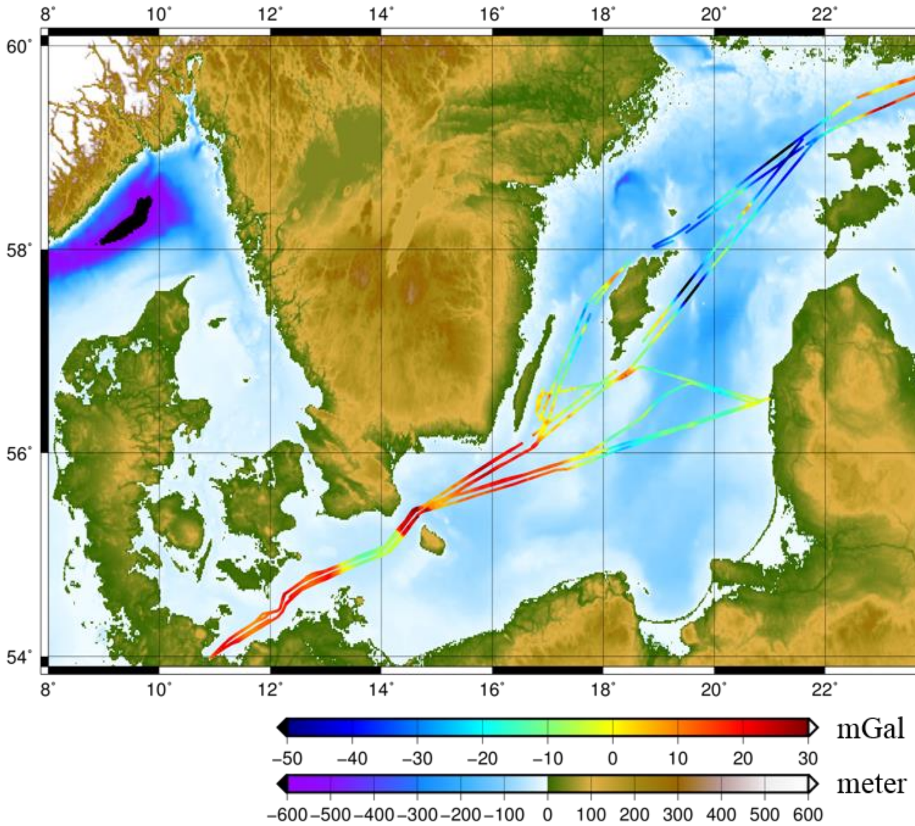

Figure 10. Gravity disturbances retrieved from the two ferry campaigns with the ETOPO1 bathymetry plotted in the background. The results from the two ferry campaigns are in good agreement with each other in the common areas.

4.2. Cross-over Analyses

The final gravity disturbance values retrieved from the two ferry campaigns are compared at the cross over (XO) points with repeating measurements from the same campaign, with the other ferry campaign as well as with three previous dedicated campaigns results. The XO differences are used not only to assess the quality of the campaign results but also to assess the accuracy of the drift estimate. The Generic Mapping Tools' x2sys_cross script (Wessel 2010; Wessel et al. 2013) is used to extract the crossover points either between different campaigns (external crossover points) and within the same campaign (internal crossover points) excluding the repeating measurements in the harbour.

The spatial distribution of the internal and external XO points of the ferry campaigns (both 400 second low-pass filtered) and their magnitudes are shown in **Figure 11**. Unfortunately, there are only very few internal XO points (15) in the Finnlady campaign (**Figure 11**a) since we could not include the first track in the assessment due to the noisy segments (see Section 2.2.1). Moreover, during the periods where the ferry approaches the harbour in Helsinki, we clearly saw that the changes in the speed of the ferry influence the measurements and accordingly the cross-over differences. Consequently, the XO points close to the land cannot be used for validation purposes and the measurements in these regions were also eliminated.

The statistics shown in **Table 2**a summarise the internal and external XO point differences of the 400 second low-pass filtered Finnlady campaign final products. The agreement within the Finnlady campaign itself and w.r.t. the Urd ferry campaign is within 1 mGal. The comparisons w.r.t. dedicated campaigns indicate a notable agreement although the Deneb2018 campaign shares only 4 XO points with Finnlady measurements. Similar comparisons are performed also for the datasets (with the same low-pass filter applied) that are corrected for the kinematic vertical acceleration and dynamical effects. The standard deviations of XO point residuals are indicated in **Table 2**a in parenthesis. The results based on the corrected series give slightly (~0.1 mGal) worse results, confirming the assessment that these corrections are not relevant.

The Finnlady campaign results retrieved from a shorter cut-off wavelength (300 seconds) are summarised in **Table 2**b. Even though there is a slightly better agreement among the Finnlady campaign measurements, the comparisons w.r.t. the three dedicated campaigns indicate slightly worse results. Based on the XO point analyses we cannot draw a clear conclusion due to the small number of shared points. Moreover, in order to properly check the quality of the final results, the number of XO points and their distribution in time and spatial domain should be better than is the case in our Finnlady campaign. As mentioned in Section 3.1, to be consistent with our other campaigns, we used 400 second cut-off wavelength in this example as well.

For the Urd2017 campaign, after removing five outliers (due to turns, speed changes and bad conditions), results are shown in **Figure 11**b for the 48 remaining XO points. Apart from the two points showing larger differences (in red), the colour scale indicates a range of -0.5 to 0.5 mGal which shows the consistency between the measurements collected at the same points (internal) during the campaign. **Figure 11**c shows the distribution of the XO points (external) and the differences between the two campaigns at 38 XO points. The XO analyses results for the Urd Ferry campaign are summarised in **Table 3**. The results indicate a good agreement within 1 mGal and suggest that the ferry campaign results are compatible with dedicated campaigns. The results can further be improved by extending the outlier detection range and/or criteria.

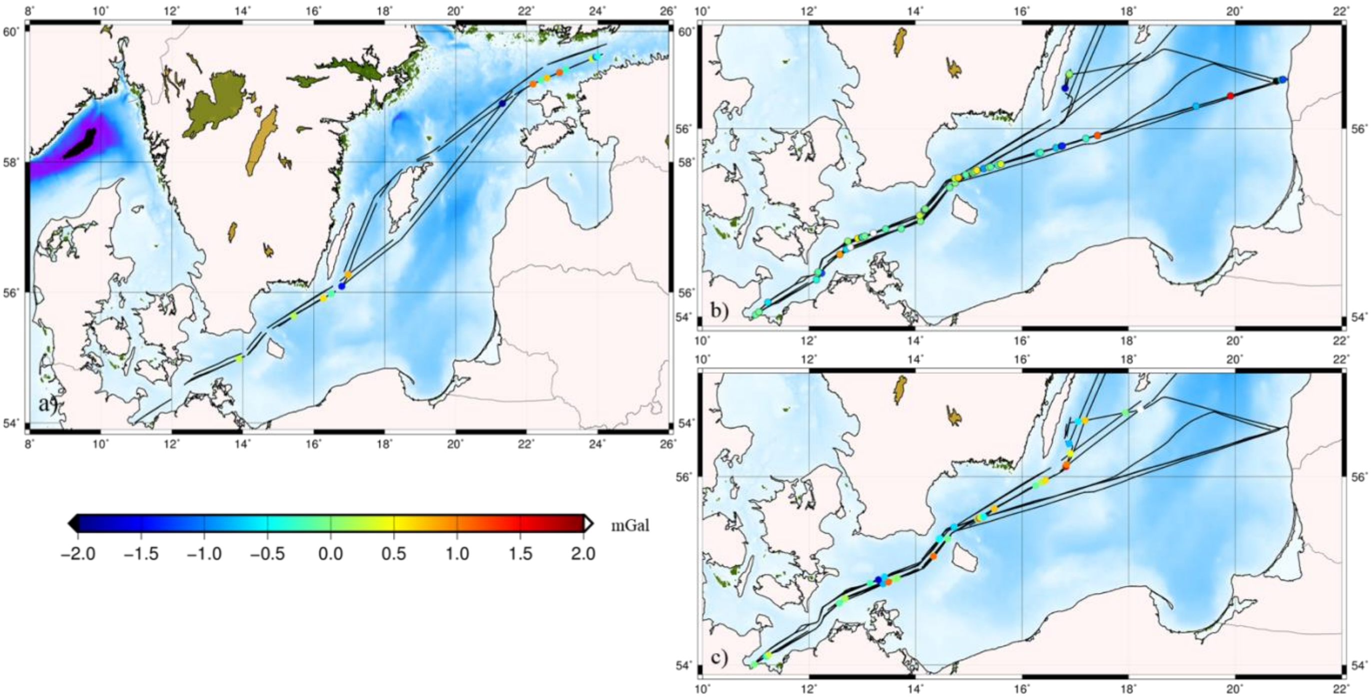

Figure 11. Crossover point differences shown in colour scale a) XO point differences within the Finnlady campaign (internal) b) XO point differences within the Urd Campaign (internal), c) XO point differences between the Finnlady and Urd campaigns (external).

Table 2. Statistics of crossover point differences for the Finnlady campaign (internal) and w.r.t. the Urd and three dedicated campaigns (external), a) 400 seconds cut-off wavelength, values in parentheses refer to the XO residuals of the series where the two corrections (kinematic vertical and dynamical) are applied, b) 300 seconds cut-off wavelength. The values are given in mGal.

a)	**Finnlady2018 (15 XO)**	**Urd2017 (37 XO)**	**Deneb2016 (17 XO)**	**Deneb2017 (20 XO)**	**Deneb2018 (4 XO)**
max	1.12	1.94	1.53	0.80	0.59
min	-1.95	-1.91	-0.34	-0.59	-0.26
mean	-0.02	-0.02	0.44	-0.12	0.16
std	**0.91** (0.90)	**0.81** (0.93)	**0.57** (0.66)	**0.39** (0.49)	**0.35** (0.38)

b)	**Finnlady2018_300s (25 XO)**	**Urd2017 (40 XO)**	**Deneb2016 (17 XO)**	**Deneb2017 (20 XO)**	**Deneb2018 (4 XO)**
max	1.88	2.49	1.72	0.66	1.04
min	-1.55	-1.67	-0.82	-1.60	-0.01
mean	-0.03	0.16	0.10	-0.25	0.62
std	**0.80**	**0.99**	**0.68**	**0.52**	**0.46**

Table 3. Statistics of crossover point differences for the Urd campaign (internal) and w.r.t. the Finnlady and dedicated campaigns (external). The values are given in mGal.

	Urd2017 (48 XO)	**Finnlady2018 (38 XO)**	**Deneb2016 (49 XO)**	**Deneb2017 (45 XO)**	**Deneb2018 (16 XO)**
max	2.04	1.94	2.21	1.76	1.45
min	-2.77	-1.91	-1.42	-1.37	-1.49
mean	-0.10	-0.02	0.08	-0.09	0.15
std	**0.88**	**0.81**	**0.68**	**0.59**	**0.86**

4.3. Representation and Publication of the Final Products

Common practice in geodesy is to downward continue the gravity data to the geoidal surface. However, the Earth gravity field is a 3-dimensional function and to compute (approximately) a gravity field model at any surface from gravity measurements it is necessary and sufficient to know the 3D-positions (e.g. longitude, latitude, and ellipsoidal height) of the measurements. We find it more useful to provide to the community the measurements at the points where they are measured rather than reducing them to a common surface with approximative transformation procedures. Accordingly, we did not lower our data to the mean sea level, but we retrieve and deliver the absolute gravity values at instrument elevation. The gravity field model computed from the measurements can then be used to calculate 3D-gravity functionals (e.g. gravity, gravity anomaly, gravity disturbance) at desired surface (e.g. Earth's surface or the geoid).

The final datasets of both ferry campaigns have been published with GFZ Data Services (Ince et al., 2020) and are publicly accessible (see draft version at: http://pmd.gfz-potsdam.de/panmetaworks/review/f964bddd75c9c8ea0a02d9ae805cf1545b8e9837fb569733a32ae7b719475887/). There, the data records are given along the measurement tracks in terms of absolute gravity values at ellipsoidal height of the instrumental sensor.

5. Conclusions

Gravity measurements on non-survey vessels such as commercial ferries hold potential for cost-efficient possibilities to expand the coverage of marine gravity observations. In this study we analysed gravity measurements taken onboard two ferry lines, to see how their accuracy compares with that of dedicated campaigns. In particular, we investigate corrections for kinematic vertical acceleration that is due to the motion of the ferry in vertical direction and dynamical effects which is sum of the horizontal accelerations and cross-coupling effects that are due the instrumental imperfection. We analysed the ferry campaign measurements with and without the two corrections applied and investigated their influence on the final products.

The kinematic vertical acceleration correction was computed by Li et al. (2019). Even though two antennae were installed onboard, due to the problems faced in one of the antennae solutions, the kinematic vertical accelerations are computed using solutions from one antenna only. The computed corrections are found not accurate enough to be introduced in the routine data processing. We believe the corrections can be improved using the solutions retrieved from both antennae. Nevertheless, in these two particular cases that we investigated, we do not recommend applying the kinematic acceleration corrections.

On the other hand, the dynamical effect correction, to remove the residual effect of cross-coupling of the vertical and horizontal axes of the gravimeter, is too small to be taken into account. That is because the influence of the oscillation of the ferry is already minimised by the instrument's internal construction with the two quartz torsion sensors. Based on our investigations, the same data processing as in previous campaigns performed on survey vessels can be applied to the ferry campaigns without any need for modification or introduction of additional correction.

As applied in our other campaigns, the drift for the ferry campaigns was estimated from measurements in harbour tie points. The first track of the Finnlady campaign resulted in a drift correction that was inconsistent with other tracks and with the estimate from the manufacturer. The reasons for such drift inconsistencies are not clear. Unknown effects of temperature changes and influence of large accelerations on the gravity sensor (liquid) could cause this. For long ferry-tracks, a stable linear drift behaviour of the gravimeter is important. The drift estimation is sensitive to the input data and therefore it should be performed carefully using quiet time measurements in the harbours.

Based on our findings which are presented in this contribution, we can conclude that the same data processing scheme that is proven to work for the dedicated shipborne campaigns can be applied to the ferry campaigns as well. From the data analysis, we can conclude that the results delivered by the ferry campaigns are of good quality for a much lower cost with an accuracy level comparable to the dedicated gravity campaigns onboard survey vessels. This is an encouraging result which suggests that conducting gravity measurements on ferry lines in different parts of the world such as in the North Sea can make a useful contribution to marine gravimetry.

Acknowledgements

The two ferry campaigns were performed within the Finalising Surveys for the Baltic Motorways of the Sea (FAMOS) project that was supported by the European Commission within the Connecting Europe Facility (CEF) Transport Sector under the Grants No. INEA/CEF/TRAN/M2014/1027106 and INEA/CEF/TRAN/M2015/1124688. GFZ's activities in the ferry campaigns as well as the above-mentioned dedicated campaigns were financially supported for 50% from the FAMOS project. The implementation of these ferry campaigns was made possible by the support of Finish Transport Agency (FTA), Maritime Administration of Latvia (MAL) and German Federal Maritime and Hydrographic Agency (BSH). The shipping companies Stena Line Scandinavia AB Göteborg and Finnlines Oyj Helsinki are acknowledged for supporting our project. The crews on the ferry liners are thanked for their help and understanding during the campaigns and for their hospitality onboard. Mirjam Bilker-Koivula and Hannu Ruotsalainen from Finnish Geospatial Research Institute (FGI) are acknowledged for providing the gravity reference in Helsinki, and Jan Müller and Andreas Reinhold from Federal Agency for Cartography and Geodesy (BKG) for providing the gravity reference and gradient measurements in Travemünde. Finally, the two reviewers are acknowledged for their feedback on an earlier version of this paper. The final processed dataset (Ince et al. 2020) can be downloaded from GFZ Data Services. http://doi.org/10.5880/GFZ.1.2.2020.001.

References

Ågren, J., G. Liebsch, J. Mononen, L. Jakobsson, B. Hell, J. Schwabe, and W. Ellmer. 2016a. On the definition and realisation of the Baltic Sea Chart Datum 2000. In 1st Joint Commission 2 and IGFS Meeting International Symposium on Gravity, Geoid and Height Systems. Thessaloniki, Greece (pp. 19-23).

Ågren, J., G. Strykowski, M. Bilker-Koivula, O. Omang, S. Märdla, R. Forsberg, A. Ellmann, T. Oja, I. Liepins, E. Parseliunas et al. 2016b. The NKG2015 gravimetric geoid model for the Nordic-Baltic region. Gravity, Geoid and Height Systems (GGHS) 2016, September 19–23, Thessaloniki, Greece.

Ågren, J. et al. 2019. FAMOS Activity 2, Harmonising vertical datum (FAMOS Freja), Improving vessel navigation for the future (FAMOS Odin), BSHC CDWG meeting, Ålborg, 5-6 February, http://www.bshc.pro/media/documents/CDWG/CDWG11+Presentation_FAMOS_Odin_final_act21-22_Agren_CDWG2019.pdf.

Barthelmes, F., S. Petrovic, C. Foerste, B. Lu, G. Liebsch, J. Schwabe, and W. Ellmer. 2016. Experiences from air- and ship-borne gravity missions. In 1st Joint Commission 2 and IGFS Meeting International Symposium on Gravity, Geoid and Height Systems. Thessaloniki, Greece, poster presentation.

Bilker-Koivula, M., J. Mononen, C. Förste, F. Barthelmes, J. Ågren, B. Lu, and T. Saari. 2017. Improving the geoid model for future GNSS-based navigation in the Baltic Sea. FIG Working Week 2017, Helsinki, Finland, May-June, 2017. Accessed Feb 4, 2020.

Bidel, Y., N. Zahzam, C. Blanchard, A. Bonnin, M. Cadore, A. Bresson, D. Rouxel, and Lequentrec-Lalancette M.F. 2018. Absolute marine gravimetry with matter-wave interferometry. Nature communications, 9(1), 627.

Bidel, Y., N. Zahzam, A. Bresson, C. Blanchard, M. Cadoret, A.V. Olesen, and R. Forsberg. 2020. J Geod, 94: 20. https://doi.org/10.1007/s00190-020-01350-2

Blazhnov, B. 2002. Integrated mobile gravimetric system-development and test results. In: 9th Saint Petersburg international conference on integrated navigation systems, St. Petersburg, pp 223–232

Böhm, J., B. Werl, and H. Schuh. 2006. Troposphere mapping functions for GPS and VLBI from ECMWF operational analysis data, Journal of Geophysical Research Vol. 111, B02406, doi: 10.1029/2005JB003629

ETOPO: ETOPO1 Global Relief Model, doi:10.7289/V5C8276M.

Förste C, Bruinsma S, Abrikosov O, Lemoine JM, Marty J, Flechtner F, Balmino G, Barthelmes F, Biancale R (2014) EIGEN-6C4 The latest combined global gravity field model including GOCE data up to degree and order 2190 of GFZ Potsdam and GRGS Toulouse. GFZ Data Services. http://doi.org/10.5880/icgem.2015.1.

Ince, E. S., C. Förste, F. Barthelmes, and H. Pflug. 2020. Ferry Gravimetry Data from the EU FAMOS project, GFZ Data Services. http://doi.org/10.5880/GFZ.1.2.2020.001.

Jekeli, C. 2001. Inertial navigation systems with geodetic applications. Walter de Gruyter, Berlin

Johann, F. D. Becker, M. Becker, E. S. Ince. 2020. Multi-Scenario Evaluation of the Direct Method in Strapdown Airborne and Shipborne Gravimetry." 5th IAG Symposium on Terrestrial Gravimetry: Static and Mobile Measurements. International Association of Geodesy Symposia, Springer, [in review].

Krasnov, A. A., L. P. Nesenyuk, V. G. Peshekhonov, A.V. Sokolov, and L.S. Elinson. 2011a. Integrated marine gravimetric system. Development and operation results. Gyroscopy and Navigation, 2(2), 75-81.

Krasnov, A. A., A. V. Sokolov, and S.V. Usov. 2011b. Modern equipment and methods for gravity investigation in hard-to-reach regions. Gyroscopy and Navigation, 2(3), 178.

Krasnov, A. A., A. V. Sokolov, and L.S. Elinson. 2014. Operational experience with the Chekan-AM gravimeters. Gyroscopy and Navigation, 5(3), 181-185.

Krasnov, A., and Sokolov, A. 2015. A modern software system of a mobile Chekan-AM gravimeter. Gyroscopy Navig 6(4):278–287

Jentzsch, G., R. Schulz, and A. Weise. 2018. Automated Burris gravity meter for single and continuous observation, Geodesy and Geodynamics 9 (2018) 204e209, https://doi.org/10.1016/j.geog.2017.09.007

Li, M., K. H., Neumayer, F. Flechtner, B. Lu, C. Förste, K. He, and T. Xu. 2019. Performance assessment of multi-GNSS precise velocity and acceleration determination over Antarctica. Journal of Navigation, 72(1), pp 1-18, doi:10.1017/S0373463318000656.

Lu, B., F. Barthelmes, S. Petrovic, C. Förste, F. Flechtner, Z. Luo, K. He, and M. Li. 2017. Airborne gravimetry of GEOHALO mission: data procesisng and gravity field modelling, Journal of Geophysical Research: Solid Earth, 122(12), 10-586.

Lu, B., F. Barthelmes, L. Min, C. Förste, E. S. Ince, S. Petrovic, F. Flechtner, J. Schwabe, Z. Luo, B. Zhong, and K. He. 2019. Shipborne gravimetry in the Baltic Sea: data processing strategies, crucial findings and preliminary geoid determination tests. Journal of Geodesy, Volume 93, Issue 7, pp 1059–1071, https://doi.org/10.1007/s00190-018-01225-7.

Märdla, S., J. Ågren, G. Strykowski, T. Oja, A. Ellmann, R. Forsberg,... & J. Kaminskis. 2017. From discrete gravity survey data to a high-resolution gravity field representation in the Nordic-Baltic region. Marine geodesy, 40(6), 416-453.

Michalak, G., D. König, K. H. Neumayer, and C. Dahle. 2014. Improvement in GPS Orbit Determination at GFZ. – In Flechtner, F. Sneeuw, N. and Schuh, W.-D. (Eds.) Observation of the System Earth from SpaceCHAMP, GRACE, GOCE and future missions, GEOTECHNOLOGIEN Science Report No. 20, pp. 9-17. Springer, Berlin, Heidelberg. DOI 10.1007/978-3-642-32135-1

Nordman, M., J. Kuokkanen, M. Bilker-Koivula, H. Koivula, P. Häkli, and S. Lahtinen. 2018. Geoid Validation on the Baltic Sea Using Ship-borne GNSS Data. Marine Geodesy, 41(5), 457-476.

Petrovic, S., F. Barthelmes, and H. Pflug. 2016: Airborne and Shipborne Gravimetry at GFZ with Emphasis on the GEOHALO Project. - In: Rizos, C., Willis, P.(Eds.), IAG 150 Years: Proceedings of the IAG Scientific Assembly in Postdam, Germany, 2013, (International Association of Geodesy Symposia ; 143), Springer, pp. 313-322. DOI: http://doi.org/DOI:10.1007/1345_2015_17.

Scintrex. 2018. CG-6 Autograv Gravity Meter Operation Manual, https://scintrexltd.com/wp-content/uploads/2018/04/CG-6-Operations-Manual-RevB.pdf

Sokolov, A. 2011. High accuracy airborne gravity measurements. Methods and equipment. In: IFAC proceedings volumes (IFACPapersOnline), proceedings 18th IFAC world congress, pp 1889–1891

Sokolov, A. V., A. A. Krasnov, and L. K. Zheleznyak. 2019. Improving the Accuracy of Marine Gravimeters. Gyroscopy and Navigation, 10(3), 155-160.

Varbla, S., A. Ellmann, S. Märdla, and A. Gruno. 2017. Assessment of marine geoid models by ship-borne GNSS profiles. Geodesy and Cartography, 43(2), 41-49.

Varbla, S., A. Ellmann, S.and Delpeche-Ellmann N. 2020. Validation of marine geoid models by utilizing hyrodynamic model and shipborne GNSS profiles, Marine Geodesy, 1-29.

Weatherall, P., K. M. Marks, M. Jakobsson, T. Schmitt, S. Tani, J. E. Arndt, M. Rovere, D. Chayes, V. Ferrini, and R. Wigley. 2015. A new digital bathymetric model of the world's oceans. Earth and Space Science, 2(8), 331-345.

Wessel, P. 2010. Tools for analyzing intersecting tracks: the x2sys package. Computers & Geosciences, 36(3), 348-354.

Wessel, P., W. H. Smith, R. Scharroo, J. Luis, and F. Wobbe. 2013. Generic mapping tools: improved version released. Eos, Transactions American Geophysical Union, 94(45), 409-410.

Zheleznyak, L. K., A. A. Krasnov, and A. V. Sokolov. 2010. Effect of the inertial accelerations on the accuracy of the CHEKAN-AM gravimeter. Izvestiya, Physics of the Solid Earth, 46(7), 580-583.

Zheleznyak, L. K. 2010b. The accuracy of measurements by the CHEKAN-AM gravity system at sea. Izvestiya, Physics of the Solid Earth, 46(11), 1000-1003